Chinese Chemical Letters 32 (2021) 2443–2447

Contents lists available at ScienceDirect

Chinese Chemical Letters

journal homepage: www.elsevier.com/locate/cclet

Communication

Selective sensing of Cr^{VI} and Fe^{III} ions in aqueous solution by an exceptionally stable Tb^{III}-organic framework with an AIE-active ligand

Jing-Jing Pang[a], Rui-Huan Du[a], Xin Lian[a], Zhao-Quan Yao[a,*], Jian Xu[a,*], Xian-He Bu[a,b]

[a] School of Materials Science and Engineering, National Institute for Advanced Materials, Tianjin Key Laboratory of Metal and Molecule-Based Material Chemistry, Nankai University, Tianjin 300350, China
[b] State Key Laboratory of Elemento-Organic Chemistry, College of Chemistry, Nankai University, Tianjin 300071, China

ARTICLE INFO

Article history:
Received 20 December 2020
Received in revised form 14 January 2021
Accepted 19 January 2021
Available online 27 January 2021

Keywords:
Lanthanide metal-organic framework
Aggregation-induced emission
Heavy metal ions
Selective luminescence sensing
Aqueous-phase sensing

ABSTRACT

We herein report a new lanthanide metal-organic framework (MOF) that exhibits excellent chemical stability, especially in the aqueous solution over a wide pH range from 1 to 14. In contrast to many reported lanthanide MOFs, this Tb-based MOF emits cyan fluorescence inherited from the integrated AIE-active ligand, rather than Ln^{3+} ions. More remarkably, its fluorescence signal features a highly selective and sensitive "turn-off" response toward CrO_4^{2-}, $Cr_2O_7^{2-}$ and Fe^{3+} ions, highlighted with the low detection limits down to 68.18, 69.85 and 138.8 ppm, respectively. Thus, the exceptional structural stability and sensing performance render this material able to be a superior luminescent sensor for heavy metal ions in wastewater.

To date, heavy metal ions are still one of the most common sources of water contamination, posing a severe poisoning risk to human beings and animals, and the booming industrialization has continued to aggravate this situation. In this context, hexavalent chromium (Cr^{VI}) is one of the well-known toxic heavy metal pollutants [1–6]. The extensive use of Cr^{VI} in industry would inevitably cause leakage accidents and bring hazardous environmental pollutants in the form of $Cr_2O_7^{2-}$ or CrO_4^{2-} anion. Likewise, iron as one of the most important metals used by modern industry and technology is an essential trace element in the biochemical processes, such as blood transmission and oxygen storage [7,8]. For human health, either the deficiency or the overload of Fe^{III} ion may induce a variety of disorders, including hemochromatosis, anemia, liver damage, diabetes, heart failure, and Parkinson's disease [9,10].

At present, the prevailing detection techniques for heavy metal ions mainly include inductively coupled plasma mass spectroscopy (ICP-MS), atomic absorption spectroscopy, and electrochemical analysis [2,11–13]. However, all of these approaches are high cost, time consuming and often require expensive, non-portable apparatus. Therefore, for the sake of human health, it is highly demandable to develop a more convenient and low-cost method for the sensitive detection of heavy metal ions, especially in the aqueous phase.

Luminescence sensing is a potential solution due to its ready operability, ease of visualization, and quick response [10]. In this regard, metal-organic frameworks (MOFs) held together by the coordination bonds between metal ions/clusters and organic ligands are conceived of as a new promising class of sensing materials [14,15]. The almost infinite combinations of organic and inorganic moieties could endow them with designable pore structures and good feasibility in a wide array of applications, such as catalysis [16–18], gas storage and separation [19–22], photovoltaic conversion [23], magnetism [24,25], conductivity [26], polymerization [27–29], as well as sensing [30–39]. However, from an application perspective, a majority of MOF-based sensors are known to be intrinsically unstable in the aqueous solutions, especially under strong acidic or basic condition, greatly limiting their application scope [40].

Besides that, for MOFs, their luminescence can derive from metal nodes, organic linkers or both [41]. Compared to inorganic metal components, a huge diversity of organic ligands makes much more room for the engineering of high-luminescence materials with excellent sensing ability. Recently, employing a special kind of organic luminogens with aggregation-induced emission (AIE) activity to construct luminescent MOFs has aroused much attention. In general, by virtue of coordinative immobilization of the AIE linkers in a rigid MOF matrix, the nonradiative dissipation of these linkers can be efficiently reduced through suppressing their intramolecular rotation, vibration and motion, thus beneficial to promoting the luminescence efficiency by a MOF-promoted AIE effect.

* Corresponding authors.
E-mail addresses: lawyer185@163.com (Z.-Q. Yao), jxu@nankai.edu.cn (J. Xu).

https://doi.org/10.1016/j.cclet.2021.01.040

Bearing this in mind, we herein modify a celebrated AIE-active molecule, tetraphenylethene (TPE), as the target emissive ligand, as TPE has been widely used as fluorescent sensors, bio-imaging materials, *etc.* [42], and also been employed in fabricating MOFs with excellent photophysical properties [43–52]. By solvothermal reaction of this TPE-based organic linker, 4',4''',4'''''',4''''''''-(ethene-1,1,2,2-tetrayl)tetrakis(([1,1′-biphenyl]-4-carboxylic acid)) (namely, H_4ETTC) with Tb^{3+} ion, we obtain a new luminescent MOF with the formula of $\{H_3O{\cdot}[Tb(H_2O)_2(ETTC)]\}$ (namely, **1**). The powder X-ray diffraction (PXRD) pattern of the as-synthesized sample of **1** matches well with the simulated result based on the single crystal data, validating its crystallinity and phase purity (Fig. S5 in Supporting information). This complex possesses high coordination number and strong coordination bond between carboxyl groups and Ln^{3+} ion. As a result, it exhibits exceptional structural stability in the aqueous solution over a wide pH range of 1–14. Interestingly, this lanthanide MOF emits the H_4ETTC-based fluorescence, rather than the characteristic green light of Tb^{3+} ion, due to the absence of the antenna effect [53]. Further luminescence studies reveal that **1** displays a highly selective and sensitive quenching response to Cr^{VI} anions and Fe^{III} cation in the aqueous solutions. In addition, this sensor material has a good recyclability and anti-interference ability. Obviously, all of these merits render this material able to be a promising candidate sensor for the detection of $Cr_2O_7^{2-}/CrO_4^{2-}$ and Fe^{3+} ions in wastewater.

Single-crystal X-ray diffraction analysis reveals that **1** crystallizes in the tetragonal space group $P4_12$ and the asymmetric unit consists of one independent Tb^{3+} ion, a quarter of the H_4ETTC ligand, and two coordinated H_2O molecules (Fig. 1a). Each Tb^{3+} ion is ten-coordinated by four carboxyl groups from four individual $ETTC^{4-}$ ligands and two water molecules, yielding an octahedral node. The coordination configuration between the carboxyl groups and the Tb^{3+} ion can be viewed as four propeller-shaped blades (Fig. S6 in Supporting information). In **1**, each mononuclear Tb node connects four bidentate carboxyl groups from four $ETTC^{4-}$ linkers, while each $ETTC^{4-}$ ligand links four Tb nodes to extend into a two-dimensional (2D) network with the rhombic window of 22 Å × 14 Å in size (Figs. 1b and c). From the viewpoint of topology, the Tb monomer can be simplified as a 4-connected node, and the $ETTC^{4-}$ ligand can be viewed as a 4-connected linker. Thus, the 2D layer can be identified as a 4,4-connected net with the *sql* topology (Fig. 1d). Further, one set of parallel 2D nets are displaced with each other by 7.1 Å in an AB stacking mode and intersect vertically with another set of parallel 2D layers to generate a 2-fold interpenetrated structure. And these interpenetrated 2D layers encompass the 1D square channels with an aperture size of 2.5 Å × 2.5 Å (Figs. 1e and f). Overall, this framework exhibits a 2D-3D inclined interpenetrated structure [54–57].

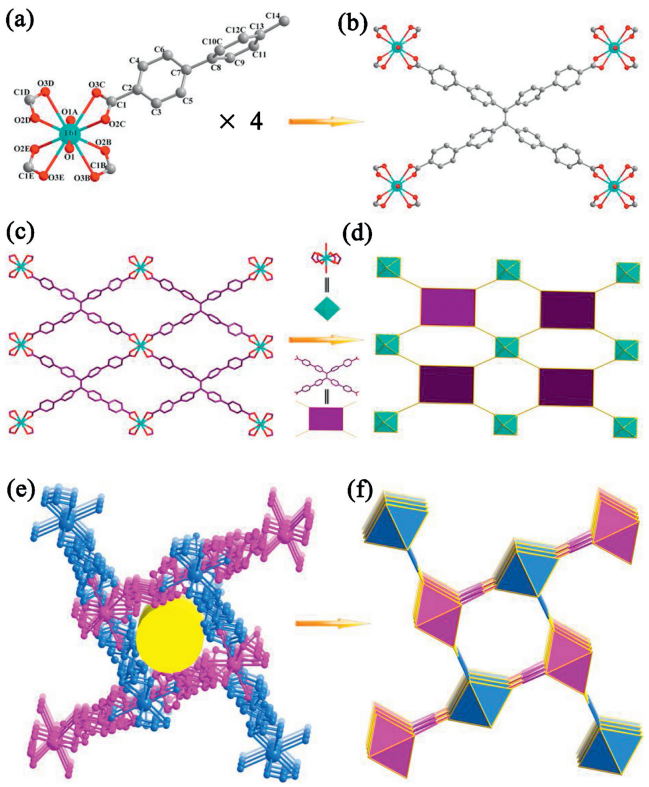

Fig. 1. (a) The asymmetric unit of **1** (A = −y, −x, −z; B = y, x, −z; C = −x, −y, z). (b) The coordination environment of the $ETTC^{4-}$ ligand in **1**. (c) The 2D layer in **1** with the *sql* topology. (d) The simplified 2D layer. (e) The two-fold interpenetrated structure of **1** with the 1D rhombic channels running along the *c* direction. (f) The simplified two-fold interpenetrated structure in **1**. All the hydrogen atoms are omitted for clarity.

The stability performance is one of the most important prerequisites for practical applications of chemosensors. After the treatment of exchanging DMAc with EtOH for 2 days, we conduct the thermogravimetric analysis (TGA) on the activated sample of **1**. The result indicates that its framework does not collapse unless the temperature reaches above 450 °C, higher than that of many reported MOFs (Fig. S7 in Supporting information). Further, the variable temperature PXRD tests confirm that **1** can retain its crystallinity until 340 °C (Fig. S8 in Supporting information). On the other hand, we also examine the chemical stability of **1** by immersing the as-synthesized sample (10 mg) in a series of common organic solvents (10 mL; *e.g.*, DMF, MeOH, EtOH, THF, CH_2Cl_2, CH_3CN, acetone and H_2O) for 2 days, and in the aqueous solutions (20 mL) with pH values ranging from 1 to 14 for 4 days. Consequently, all the PXRD peaks are well remained (Fig. 2), hinting that this MOF can maintain its crystallinity and structural regularity in a broad range of chemical environments. To our knowledge, such a degree of structural stability is rather rare in MOF chemistry and it will undoubtedly pave the way to a wide scope of applications.

Upon a 365 nm excitation, the as-obtained yellow-green block crystal of **1** emits a bright fluorescence with the maximum around 477 nm (Fig. S9 in Supporting information), which is blue-shifted by 50 nm relative to that of pure H_4ETTC ligand (527 nm) [58]. This is very common for TPE-based MOFs [34,36], as it indicates a more twisted nonplanar structure of TPE moiety in rigid MOF frameworks (Fig. S10 in Supporting information), due to the hinge effect of metal-ligand coordination. It is worth noting that many reported lanthanide MOFs exhibit the characteristic fluorescence of Ln^{3+} ions, which is sensitized by the conjugated ligand *via* the "antenna effect". According to the Reinhold's empirical rule, to invoke the antenna effect, not only is the energy gap between the singlet- and triplet-state of the ligand required to be larger than 5000 cm^{-1}, but also the energy gap between the triplet-state of the ligand and the excited state of Ln^{3+} ion must be larger than 3000 cm^{-1} [53,59,60]. However, for **1**, the energy of the main accepting level of Tb^{3+} ion is 20,500 cm^{-1}, while the HOMO-LUMO bandgap of H_4ETTC is only 2.49 eV (20,055 cm^{-1}) [58]. Evidently, **1** does not fulfill the theoretically lowest energy gap to activate the antenna effect and thereby emits the fluorescence derived solely from the AIE-active ligand.

Considering its strong luminescence and satisfactory water resistance, we attempt to explore the sensing ability of **1** with respect to a series of common ions in the aqueous solutions. A total of thirteen anions ($H_2PO_4^-$, F^-, MoO_4^{2-}, Cl^-, NO_3^-, CO_3^{2-}, I^-, SO_4^{2-}, WO_4^{2-}, NO_2^-, Br^-, CrO_4^{2-}, $Cr_2O_7^{2-}$) as well as twelve metal cations (Pb^{2+}, Li^+, Mg^{2+}, Zn^{2+}, Cd^{2+}, K^+, Na^+, Ca^{2+}, Ni^{2+}, Co^{2+}, Cu^{2+}, Fe^{3+}) are selected as the target analytes. For comparison, an equal amount of finely ground powder sample of **1** is dispersed into the respective

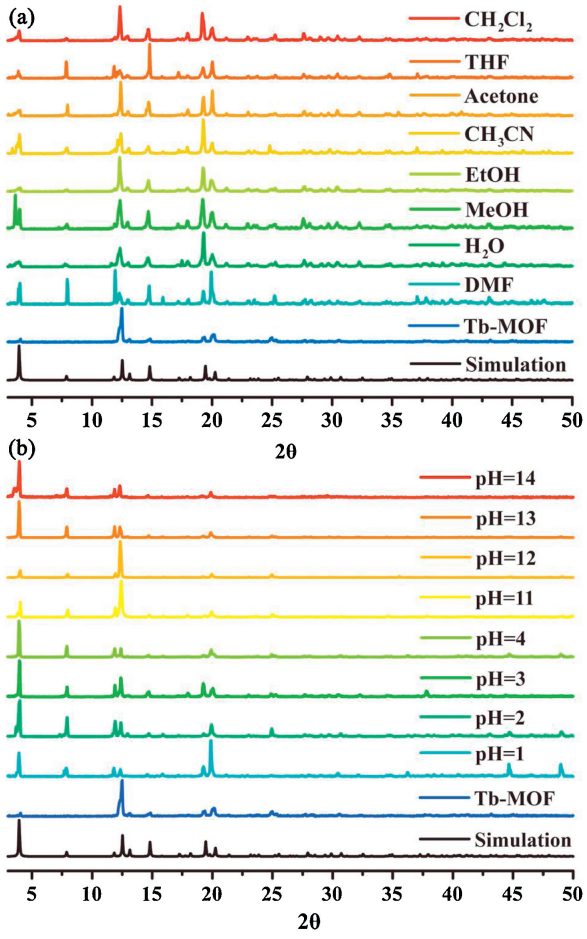

Fig. 2. (a) The PXRD patterns of **1** soaked in different organic solvents for 2 days. (b) The PXRD patterns of **1** immersed in HCl (pH 1∼4) and NaOH aqueous solutions (pH 11∼14) for 4 days.

aqueous solutions with different ions of the same concentration (10 mmol/L). Under UV illumination at 365 nm, only the fluorescence signals of the suspensions containing Fe^{3+}, CrO_4^{2-} and $Cr_2O_7^{2-}$ ions are acutely quenched, while the others display slight or no discernible changes. Such a high-contrast "turn-off" signal can be visually observed with the naked eyes (Fig. S11 in Supporting information). As estimated based on the corresponding emission spectra (Fig. S12 in Supporting information), the quenching percentages (QPs) of the suspensions containing Fe^{3+}, CrO_4^{2-} and $Cr_2O_7^{2-}$ are 99.7%, 99.8%, and 99.9%, respectively, far beyond those of the other analytes, thus indicative of highly selective quenching response of **1** toward different ions.

The sensing performances of **1** for Cr^{VI} and Fe^{III} ions are further assessed by the fluorescence titration experiments. As shown in Fig. 3, the fluorescence intensity of the suspension decreases sharply and is fully quenched when the concentration of CrO_4^{2-} reaches 31.3 ppm. The quenching trend of $Cr_2O_7^{2-}$ is akin to the case of CrO_4^{2-} and the emission is entirely dimmed when the $Cr_2O_7^{2-}$ concentration increases to 194 ppm. Slightly differing from Cr^{VI} anions, the fluorescence signal of the suspension containing Fe^{3+} moderately decreases in the early stage of the titration and entirely turns off until the Fe^{3+} concentration is above 117 ppm. We also analyze the fluorescence quenching behavior of **1** in terms of the Stern-Volmer (S-V) equation: $I_0/I = K_{sv}[Q]+1$. Herein, I_0 and I refer to the fluorescence intensity of the suspension before and after the addition of the analyte, [Q] is the molar concentration of the analyte, and K_{sv} denotes the quenching constant [61]. As shown in Fig. S13 (Supporting information), all the S-V curves for

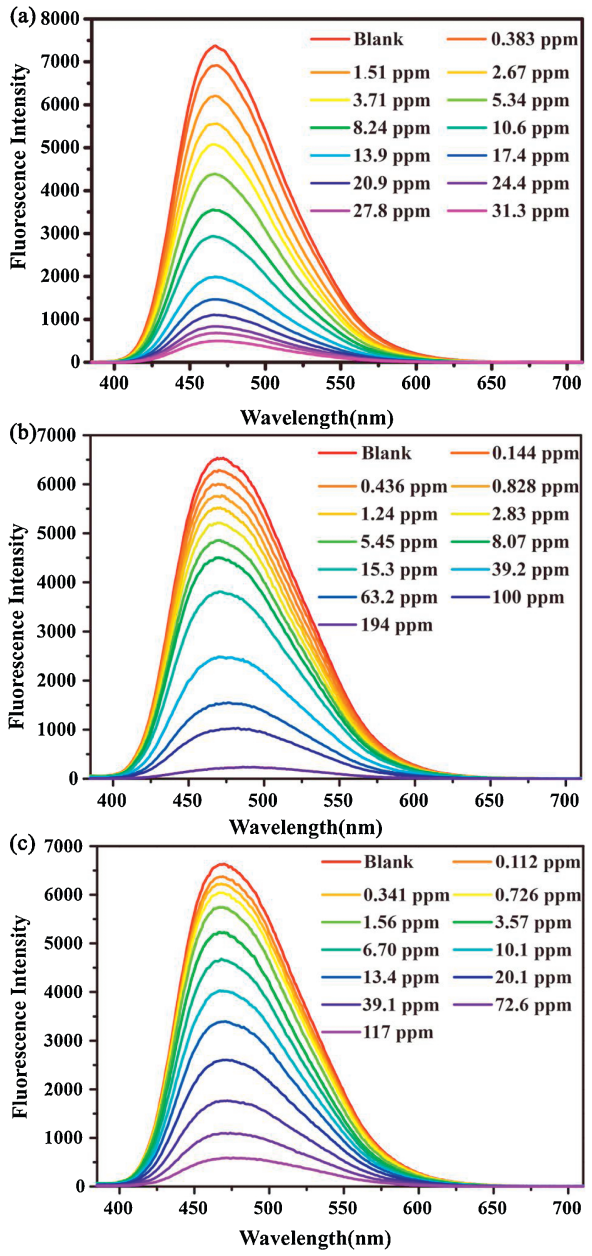

Fig. 3. Fluorescence titration experiments of **1** toward (a) CrO_4^{2-}, (b) $Cr_2O_7^{2-}$ and (c) Fe^{3+} in the aqueous solutions under a 365 nm UV lamp.

CrO_4^{2-}, $Cr_2O_7^{2-}$ and Fe^{3+} show a linear relationship in the low concentration range, with the estimated K_{sv} values being 1.48×10^4 (R^2 = 0.9925), 2.69×10^4 (R^2 = 0.9920), and 3.50×10^3 L/mol (R^2 = 0.9845), respectively, higher than many reported MOF-based sensors [62–64]. According to the formula of $3\sigma/K_{sv}$ (σ: standard error), the detection limits for CrO_4^{2-}, $Cr_2O_7^{2-}$ and Fe^{3+} are 68.18, 69.85 and 138.8 ppm, respectively, thus indicating that **1** can achieve the trace amount recognition of those heavy metal ions. In addition to high selectivity and sensitivity, *anti*-interference ability and recyclability are also important for practical application of sensors. For **1**, it is observed that the fluorescence intensity of the suspension does not significantly alter in the presence of other competing ions and reduces only after the addition of CrO_4^{2-}, $Cr_2O_7^{2-}$ and Fe^{3+} ions (Fig. S14 in Supporting information). As for its recyclability, we testify that the QP of **1** can keep almost unchanged during four consecutive sensing cycles (Fig. S15 in Supporting information). These

testaments strongly suggest **1** to be a qualified fluorescent sensor toward CrO_4^{2-}, $Cr_2O_7^{2-}$ and Fe^{3+} ions. Since now, several luminescent MOFs have been announced for detecting Cr^{VI} and Fe^{III} ions, but many of them are not applicable for the sensing in the aqueous environment, due to their intrinsically weak stability [2,3,14,65].

To unveil the underlying selective fluorescence "turn-off" mechanism of **1**, we first measure the PXRD patterns of the undissolved sample after the immersion of **1** in the aqueous solutions containing CrO_4^{2-}, $Cr_2O_7^{2-}$ and Fe^{3+} ions for 1 day. As illustrated by Fig. S16 (Supporting information), the sample exhibits good crystallinity and phase purity, revealing that its fluorescence "turn-off" sensing mechanism has no relation with framework collapse. Next, the ICP analyses are also conducted on the filtrate of the Cr^{VI} and Fe^{III}-containing solutions before and after adding **1**, respectively. The results show that none or only a negligible fraction of Cr^{VI} and Fe^{III} ions enters into the channels of **1** after 24 h (Table S3 in Supporting information), ruling out the influence of guest adsorption on the quenching behavior of **1**. Lastly, we compare the UV–vis absorption spectra of all the analytes with reference to the excitation and emission spectra of **1** (Fig. 4). Evidently, in comparison to the negligible ones of the other ions, the overlap between the absorption band of the Na_2CrO_4, $Na_2Cr_2O_7$ and $Fe(NO_3)_3$ solution and either the excitation or the emission spectrum of **1** is considerably much larger. While the former overlap (with the excitation spectrum of **1**) indicates a competitive absorption of the excitation energy between the analytes and the MOF, the latter (with the emission band of **1**) implies the occurrence of fluorescence resonance energy transfer (FRET) from the MOF to the analytes. Both the two types of spectral overlap are fully coincident with the observed QPs trend of **1** in the presence of different analytes. Therefore, we reasonably attribute the selective luminescence sensing behavior of **1** to the synergistic effect of competitive absorption and FRET mechanism [3].

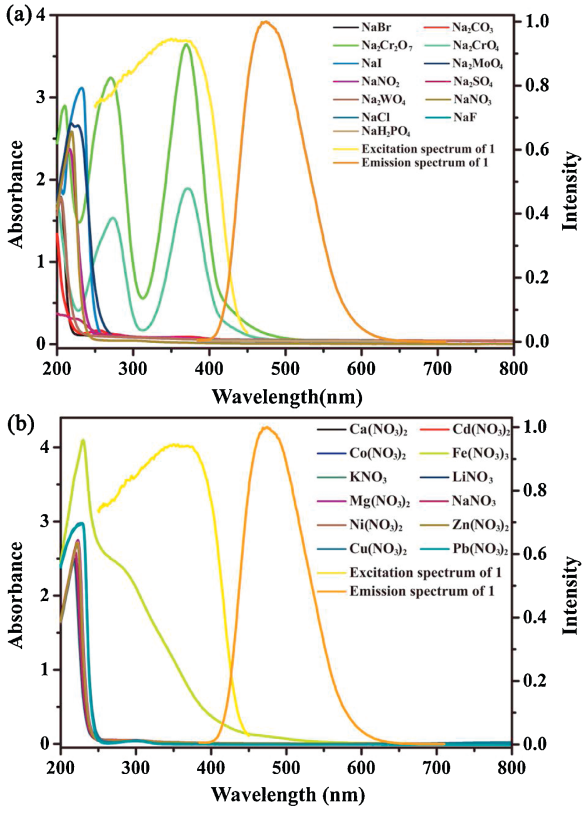

Fig. 4. The UV–vis absorption spectra of the aqueous solutions containing different anions (a) and metal cations (b) with reference to the excitation and emission spectra of **1**.

In summary, we fabricate a new luminescent lanthanide MOF by introducing an AIE-active ligand. Owing to the high coordination number of Tb^{3+} ion and its strong coordination bond with the multidentate TPE-based ligand, this MOF (**1**) exhibits excellent structural stability, which has been very rare in MOF chemistry. Unlike many reported lanthanide MOFs, **1** emits the ligand-centered fluorescence, as the excitation energy of the constituent ligand is insufficient to sensitize the fluorescence of Tb^{3+} ion. Notably, this complex displays a highly selective and sensitive fluorescence quenching toward CrO_4^{2-}, $Cr_2O_7^{2-}$ and Fe^{3+}, which can be visually observed without the interference by other common ions. Thus, considering its exceptional stability performance in the aqueous phase, we suggest that this material has a good application prospect for sensing heavy metal ions in wastewater.

Declaration of competing interest

The authors declare that they have no known competing financial interests or personal relationships that could have appeared to influence the work reported in this paper.

Acknowledgments

This work was financially supported by the National Natural Science Foundation of China (Nos. 21771113, 22001132), and China Postdoctoral Science Foundation (No. 2019M651011).

Appendix A. Supplementary data

Supplementary material related to this article can be found, in the online version, at doi:https://doi.org/10.1016/j.cclet.2021.01.040.

References

[1] C. Gogoi, H. Reinsch, S. Biswas, CrystEngComm 21 (2019) 6252–6260.
[2] W. Chen, R. Fan, J. Fan, et al., Inorg. Chem. 58 (2019) 15118–15125.
[3] Z.Q. Yao, G.Y. Li, J. Xu, T.L. Hu, X.H. Bu, Chem. Eur. J. 24 (2018) 3192–3198.
[4] W. Liu, Y. Wang, Z. Bai, et al., ACS Appl. Mater. Interfaces 9 (2017) 16448–16457.
[5] K.L. Witt, M.D. Stout, R.A. Herbert, et al., J. Toxicol. Pathol. 41 (2013) 326–342.
[6] L. Khezami, R. Capart, J. Hazard. Mater. 123 (2005) 223–231.
[7] D. Zhao, X.H. Liu, Y. Zhao, et al., J. Mater. Chem. A 5 (2017) 15797–15807.
[8] D.M. Chen, N.N. Zhang, C.S. Liu, M. Du, J. Mater. Chem. C 5 (2017) 2311–2317.
[9] S. Chen, Z. Shi, L. Qin, H. Jia, H. Zheng, Cryst. Growth Des. 17 (2016) 67–72.
[10] L.M. Hyman, K.J. Franz, Coord. Chem. Rev. 256 (2012) 2333–2356.
[11] D. Chen, L. Cao, T.L. Hanley, R.A. Caruso, Adv. Funct. Mater. 22 (2012) 1966–1971.
[12] Z. Sun, P. Liang, Microchim. Acta 162 (2008) 121–125.
[13] F. Séby, S. Charles, M. Gagean, H. Garraud, O.F.X. Donard, J. Anal. At. Spectrom. 18 (2003) 1386–1390.
[14] H.C. Zhou, J.R. Long, O.M. Yaghi, Chem. Rev. 112 (2012) 673–674.
[15] Y.P. He, Y.X. Tan, J. Zhang, Coord. Chem. Rev. 420 (2020) 213354.
[16] Q. Yang, Q. Xu, H.L. Jiang, Chem. Soc. Rev. 46 (2017) 4774–4808.
[17] F.L. Li, P.T. Wang, X.Q. Huang, et al., Angew. Chem. Int. Ed. 58 (2019) 7051–7056.
[18] F.L. Li, Q. Shao, X.Q. Huang, J.P. Lang, Angew. Chem. Int. Ed. 57 (2018) 1888–1892.
[19] H.L. Li, M. Eddaoudi, M. O'keeffe, O.M. Yaghi, Nature 402 (1999) 276–279.
[20] Y.P. He, Y.X. Tan, J. Zhang, Inorg. Chem. 52 (2013) 12758–12762.
[21] H. Li, L.B. Li, R.B. Lin, et al., EnergyChem 1 (2019) 100006.
[22] D. Liu, J.P. Lang, B.F. Abrahams, J. Am. Chem. Soc. 133 (2011) 11042–11045.
[23] V. Stavila, A.A. Talin, M.D. Allendorf, Chem. Soc. Rev. 43 (2014) 5994–6010.
[24] B. Li, H.M. Wen, Y. Cui, et al., Adv. Mater. 28 (2016) 8819–8860.
[25] E. Coronado, G.M. Espallargas, Chem. Soc. Rev. 42 (2013) 1525–1539.
[26] H.B. Wu, X.W. Lou, Sci. Adv. 3 (2017) 9252.
[27] X. Meng, H.N. Wang, S.Y. Song, H.J. Zhang, Chem. Soc. Rev. 46 (2017) 464–480.
[28] F.L. Hu, Y. Mi, C. Zhu, et al., Angew. Chem. Int. Ed. 57 (2018) 12696–12701.
[29] M.F. Wang, Y. Mi, F.L. Hu, et al., J. Am. Chem. Soc. 142 (2020) 700–704.
[30] L.E. Kreno, K. Leong, O.K. Farha, et al., Chem. Rev. 112 (2012) 1105–1125.
[31] Y. Zhang, S. Yuan, G. Day, et al., Coord. Chem. Rev. 354 (2018) 28–45.
[32] B. Yan, Acc. Chem. Res. 50 (2017) 2789–2798.
[33] W.P. Lustig, S. Mukherjee, N.D. Rudd, et al., Chem. Soc. Rev. 46 (2017) 3242–3285.
[34] D. Tian, R.Y. Chen, J. Xu, Y.W. Li, X.H. Bu, APL Mater. 2 (2014) 124111.

[35] D. Tian, Y. Li, R.Y. Chen, et al., J. Mater. Chem. A 2 (2014) 1465–1470.
[36] Y.P. He, Y.X. Tan, J. Zhang, J. Mater. Chem. C 2 (2014) 4436–4441.
[37] C.Y. Liu, X.R. Chen, H.X. Chen, et al., J. Am. Chem. Soc. 142 (2020) 6690–6697.
[38] X. Zhou, Y.X. Shi, C. Cao, et al., Cryst. Growth Des. 19 (2019) 3518–3528.
[39] T.Y. Gu, M. Dai, D.J. Young, Z.G. Ren, J.P. Lang, Inorg. Chem. 56 (2017) 4668–4678.
[40] W. Yan, C. Zhang, S. Chen, L. Han, H. Zheng, ACS Appl. Mater. Interfaces 9 (2017) 1629–1634.
[41] Y.J. Cui, J. Zhang, H.J. He, G.D. Qian, Chem. Soc. Rev. 47 (2018) 5740–5785.
[42] J. Luo, Z. Xie, J.W. Lam, et al., Chem. Commun. (2001) 1740–1741.
[43] R. Medishetty, L. Nemec, V. Nalla, et al., Angew. Chem. Int. Ed. 56 (2017) 14743–14748.
[44] X. Hu, Z. Wang, B. Lin, et al., Chem. Eur. J. 23 (2017) 8390–8394.
[45] Z. Wei, Z.Y. Gu, R.K. Arvapally, et al., J. Am. Chem. Soc. 136 (2014) 8269–8276.
[46] Q. Zhang, J. Su, D. Feng, et al., J. Am. Chem. Soc. 137 (2015) 10064–10067.
[47] N.D. Rudd, H. Wang, E.M. Fuentes-Fernandez, et al., ACS Appl. Mater. Interfaces 8 (2016) 30294–30303.
[48] X.G. Liu, H. Wang, B. Chen, et al., Chem. Commun. 51 (2015) 1677–1680.
[49] X.G. Liu, C.L. Tao, H.Q. Yu, et al., J. Mater. Chem. C 6 (2018) 2983–2988.
[50] F.M. Wang, L. Zhou, W.P. Lustig, et al., Cryst. Growth Des. 18 (2018) 5166–5173.
[51] C.X. Chen, Z.W. Wei, C.C. Cao, et al., Chem. Mater. 31 (2019) 5550–5557.
[52] Y. Zhao, Y.J. Wang, N. Wang, et al., Inorg. Chem. 58 (2019) 12700–12706.
[53] H.Q. Yin, X.Y. Wang, X.B. Yin, J. Am. Chem. Soc. 141 (2019) 15166–15173.
[54] Y.N. Gong, D.C. Zhong, T.B. Lu, CrystEngComm 18 (2016) 2596–2606.
[55] M. Meng, D.C. Zhong, T.B. Lu, CrystEngComm 13 (2011) 6794–6800.
[56] C. Ruiz-Valero, C. Cascales, B. Gómez-Lor, et al., J. Mater. Chem. 12 (2002) 3073–3077.
[57] L. Chen, K. Tan, Y.Q. Lan, et al., Chem. Commun. 48 (2012) 5919–5921.
[58] X. Wang, J. Hu, G. Zhang, S. Liu, J. Am. Chem. Soc. 136 (2014) 9890–9893.
[59] Y. Zhou, Q. Yang, D. Zhang, et al., Sens. Actuators B: Chem. 262 (2018) 137–143.
[60] S. Wu, Y. Lin, J. Liu, et al., Adv. Funct. Mater. 28 (2018) 1707169.
[61] C.H. Chen, X.S. Wang, L. Li, Y.B. Huang, R. Cao, Dalton Trans. 47 (2018) 3452–3458.
[62] X.D. Zhang, Y. Zhao, K. Chen, Y.F. Jiang, W.Y. Sun, Chem. Asian J. 14 (2019) 3620–3626.
[63] X.D. Zhang, Y. Zhao, K. Chen, et al., Dalton Trans. 47 (2018) 3958–3964.
[64] F.L. Hu, Y.X. Shi, H.H. Chen, J.P. Lang, Dalton Trans. 44 (2015) 18795–18803.
[65] Z.Q. Liu, Y. Zhao, X.D. Zhang, et al., Dalton Trans. 46 (2017) 13943–13951.